AGU PUBLICATIONS

JGR

Journal of Geophysical Research: Space Physics

RESEARCH ARTICLE
10.1002/2014JA020527

Key Points:
- Identification of auroral features possibly associated with injection signatures
- These auroral features mostly map between 7 and 40 R_J at all SIII longitudes
- The associated inward magnetic flux may account for the estimated outward flux

Supporting Information:
- Complete list of events

Correspondence to:
M. Dumont,
maite.dumont@ulg.ac.be

Citation:
Dumont, M., D. Grodent, A. Radioti, B. Bonfond, and J.-C. Gérard (2014), Jupiter's equatorward auroral features: Possible signatures of magnetospheric injections, *J. Geophys. Res. Space Physics*, *119*, 10,068–10,077, doi:10.1002/2014JA020527.

Received 3 SEP 2014
Accepted 5 DEC 2014
Accepted article online 9 DEC 2014
Published online 27 DEC 2014

Jupiter's equatorward auroral features: Possible signatures of magnetospheric injections

M. Dumont[1], D. Grodent[1], A. Radioti[1], B. Bonfond[1], and J.-C. Gérard[1]

[1]Laboratoire de Physique Atmosphérique et Planétaire, Institut d'Astrophysique et Géophysique, Université de Liège, Liège, Belgium

Abstract The present study investigates the characteristics of ultraviolet auroral features located equatorward of the main emission appearing in Hubble Space Telescope images of the northern and southern Jovian hemispheres obtained in 2000–2007. On average, one feature is observed every day, but several auroral structures are occasionally seen over a wide range of local times in the same image. Several properties of these features are analyzed, such as their location, emitted power, and lifetime. Additionally, we magnetically map the auroral features to the equatorial plane using the VIPAL model in order to compare their observed properties with those of magnetospheric injections detected by the Galileo spacecraft. The equatorward auroral features show up between the Io footpath and the main auroral emission, at all System III longitudes, in agreement with Galileo measurements. Moreover, we compare the magnetic flux associated with these features with estimates of the outgoing flux related to the radial transport of plasma in the Jovian magnetosphere, and we find that they could account for at least one third of this flux. This comparative study shows that the auroral features under study are most probably related to magnetospheric injections and thus sheds light on the processes involved in the magnetosphere-ionosphere dynamics.

1. Introduction

Plasma injections and interchange processes play a key role in the dynamics of the Jovian magnetosphere. *Mauk et al.* [1997] reported the first detection of energetic particle injection in Jupiter observed with the Energetic Particle Detector (EPD) on board the Galileo spacecraft. In the Jovian magnetosphere, which is dominated by centrifugal forces, injections are associated with radial planetward transport of hot and tenuous plasma and outward transport of cold and dense plasma from the Io plasma torus. This radial motion is most probably the result of centrifugally driven interchange events [*Siscoe and Summers*, 1981]. The centrifugal instability can trigger the interchange of the magnetic flux tubes populated by iogenic plasma with flux tubes originating in the outer magnetosphere [*Southwood and Kivelson*, 1987]. During an interchange event, the magnetic flux lost through cold plasma outflow is balanced by inward injection of hot outer magnetospheric plasma. Therefore, injection events involve high-energy particles within a colder background plasma.

Mauk et al. [1999] performed a statistical analysis of these energy-time-dispersed intensifications in the energetic ions and electrons, based on Galileo EPD data, and found that energetic particle injections are commonly observed in the Jovian magnetosphere from 9 to 27 Jovian radii (R_J ; 1 R_J = 71,492 km), at all System III longitudes and all local times. Later on, *Mauk et al.* [2002] associated an isolated equatorward patchy auroral ultraviolet emission with energetic particle injections threading the same flux tube. Nevertheless, this association is based on a single set of simultaneous observations. *Mauk et al.* [2002] proposed two mechanisms that are able to produce the auroral signatures of an injection: (1) electron pitch angle scattering and (2) electric field-aligned currents flowing along the boundary of the hot injected plasma cloud. Consisting of broadband images, the data used in this study do not allow us to differentiate between these two mechanisms. The goal of the present study is to statistically investigate the properties of the equatorward auroral emissions and establish their possible association with magnetospheric plasma injections.

Two different phenomena could be referred to as "injection" because of their association with increased intensities of energetic particles. The first one is related to the interchange instability process, which brings sparsely populated hot plasma from the outer magnetosphere toward the inner magnetosphere [e.g., *Siscoe and Summers*, 1981; *Thorne et al.*, 1997; *Mauk et al.*, 1999]. This process is thought to explain the injection

reported by *Mauk et al*. [2002]. The second phenomenon associated with an injection involves particle acceleration events related to planetward transport and heating of plasma following magnetic reconnection [*Krupp et al*., 1998].

In the frame of internally driven magnetic reconnection at Jupiter (Vasyliūnas cycle *Vasyliūnas* [1983]), magnetic flux tubes are loaded with heavy ions from iogenic plasma [*Carbary et al*., 1976; *Vasyliūnas*, 1983]. This plasma moves outward into the stretched magnetotail under the influence of centrifugal forces and pressure anisotropies [*Paranicas et al*., 1991]. When the tail becomes sufficiently stretched, Vasyliūnas-type reconnection occurs. This process creates a mass-loaded plasmoid, which is no longer constrained by the planetary magnetic field and thus quickly moves away from the planet on one hand and a heated but mass-depleted flux tube that moves planetward and dipolarizes on the other hand. Auroral polar dawn spots have been related to precipitated heated plasma injected during internally driven reconnection process at Jupiter [*Radioti et al*., 2008, 2010]. In addition to these auroral features, similar arcs and midnight spots observed in the polar auroral region were also suggested to be associated with inward moving flow released during magnetic tail reconnection without being able to determine whether reconnection, in those cases, was solar wind or internally driven [*Grodent et al*., 2008; *Radioti et al*., 2011]. Recently, *Louarn et al*. [2014] also associated radio signatures of reconnection events, occurring in the outer magnetosphere, with energetic particle injections taking place in the inner magnetodisk thus confirming the possible link between reconnection and injection.

The present study focuses on isolated equatorward auroral features showing the same appearance as the auroral signature of an injection previously observed by *Mauk et al*. [2002]. These features consist of quasi-corotating isolated structures spanning a region roughly bounded poleward by Jupiter's main emission, associated with corotation enforcement process [e.g., *Cowley and Bunce*, 2001]. *Thomsen* [2013] reviewed the dynamics of Saturn's magnetosphere and distinguished radio signatures of high-energy injections from low-energy injections. These two types of injections are observed in the same space's region, and they have some similar properties. The auroral data set that was used in the present study does not make it possible to discriminate between low-energy and high-energy events. However, if the structures studied are indeed associated with plasma injection, then the broadband images used here cannot discriminate between these two types of injections; therefore, we cannot distinguish the young auroral features from the old ones. We note that in the case of Saturn's magnetosphere, *Kennelly et al*. [2013] found that creation of injection events is preferentially taking place into the postnoon and midnight sectors. Accordingly, it is difficult for us to accurately trace back the creation region of these auroral structures. In the present study, we analyze observations of the auroral regions of Jupiter and compare them with statistical results obtained with in situ instruments. We analyze their location, emitted power, and lifetime and we compare their observed properties with those of magnetospheric injections detected by the Galileo spacecraft. Moreover, we compare the amount of magnetic flux moving toward and away from the planet in the Jovian magnetosphere. The combined use of remote and in situ observations allows us to investigate the importance of plasma transport in the Jovian magnetosphere.

2. Hubble Space Telescope Ultraviolet Observations

This study is based on a collection of 1874 high-resolution ultraviolet (UV) images obtained from 2000 to 2007 with the Advanced Camera for Surveys (ACS) and the Space Telescope Imaging Spectrograph (STIS) on board the Hubble Space Telescope (HST). Approximately 75% of the data set was obtained during a large HST campaign that lasted for a few months in 2007. During this campaign, images were captured every day during single orbits or across consecutive multiple orbits. We consider images obtained using the F115LP and the F125LP filters on ACS and the Clear and Strontium Fluoride (SrF2) filters on STIS. They are sensitive to the bright UV emissions of H_2 and H in the 115–170 nm range. The conversion from counts per second to brightness or power units is performed using the coefficients derived by *Gustin et al*. [2012].

The center position of the planet is determined by the limb fitting procedure described by *Bonfond et al*. [2009]. It allows one to project the images on a polar map fixed in System III, where structures corotating with the planet may be easily distinguished from those lagging corotation. The accuracy of the projection decreases toward the limb, where the pixels are stretched for geometrical reasons. Accordingly, we excluded from our analyses the features located less than 10° away from the limb plane. Approximately 10% of the structures were rejected by this criterion.

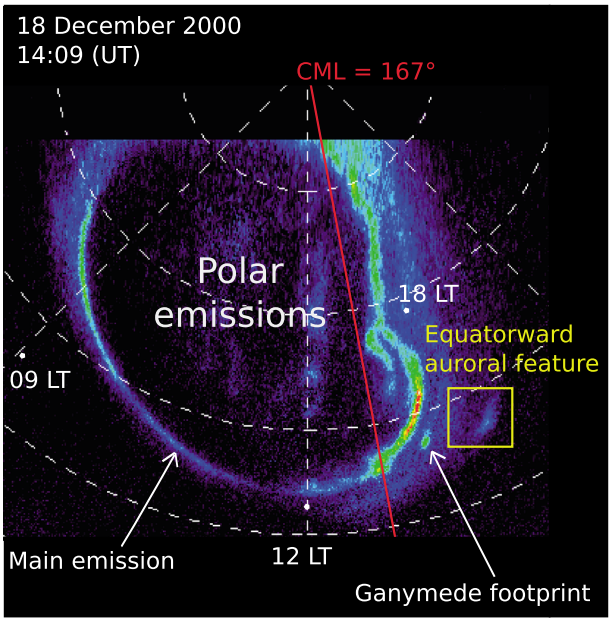

Figure 1. Polar projection of an HST/STIS image in a reference frame fixed in System III. The image shows the northern Jovian aurora on 18 December 2000 at 14:09 UT. The central meridian longitude (red line) is 167° System III. In this particular case, noon (12 LT) is approximately toward the bottom and dusk (18 LT) to the right. The main auroral features are indicated: the main emission, Ganymede footprint, polar emissions, and equatorward auroral feature. In this case, the equatorward auroral feature has a latitudinal extent of ~3 km and a longitudinal extent of ~3 km in the ionosphere.

For Earth-based observations of Jupiter's aurora, the viewing geometry of the southern Jovian aurora is less favorable than in the north. In the southern hemisphere, the magnetic pole is relatively close to the jovigraphic pole, and a limited amount of the equatorward most emission can be observed, whatever the central meridian longitude (CML). In the northern hemisphere, the magnetic dipole axis is significantly tilted relative to the spin axis, and when the dipole axis points toward the observer, only a small portion of the auroral emission is hidden beyond the limb. The downside is that a very small portion of the aurora is in sight when the dipole is pointing away. This results in a strong bias in terms of observable System III longitudes. The bias was accounted for in the present analysis which relies on a large set of 1123 images of the northern hemisphere and 751 images of the southern hemisphere. All auroral features analyzed in this study were selected to satisfy some specific criteria: they are (1) equatorward of the main emission, (2) detached from the main emission (isolated), (3) compact structures (longitudinal mean extent $<6°$ and latitudinal mean extent $<3°$) that are not secondary arcs or diffuse emissions, (4) they must evolve regardless of the rest of the auroral emission's behavior, and (5) they are not satellite footprints. Application of these criteria resulted in the identification of 130 individual UV auroral features.

Figure 1 shows the polar projection in System III coordinates of an image of the northern UV aurora obtained with STIS on 18 December 2000. In this example, the main emission [i.e., *Grodent et al.*, 2003a], the polar emissions [i.e., *Grodent et al.*, 2003b], Ganymede's footprint [i.e., *Grodent et al.*, 2009], and the region of equatorward emissions [i.e., *Radioti et al.*, 2009b] are indicated. In the latter region, an isolated patchy auroral structure is pointed out; this equatorward auroral feature fulfills the selection criteria.

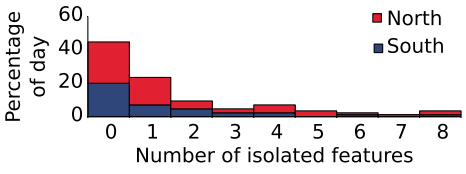

Figure 2. Histogram of isolated transient auroral structures observed in the north (red) and in the south (blue). The percentage of day correspond to the percentage of Earth day observed where the number of auroral features vary between 0 and 8. The number of auroral features varies between 0 and 8. On average, more than half of observations present one or more auroral signatures of events.

2.1. Analysis of Equatorward Isolated Auroral Structures

As mentioned above, 130 auroral features have been identified in the data set of images acquired between 2000 and 2007 (the complete list of events are available in the supporting information). In brief, these auroral emissions were observed during 52 different days in the northern hemisphere and 33 different days in the southern hemisphere, corresponding to an average number of ~1.5 auroral features per day. Figure 2 displays a histogram giving the percentage of days during which a certain number of auroral features were visible in the northern (red) and in the southern (blue) hemispheres. The median value is 1 auroral feature per day. In ~60% of the cases in the north and ~50% of the cases in the south,

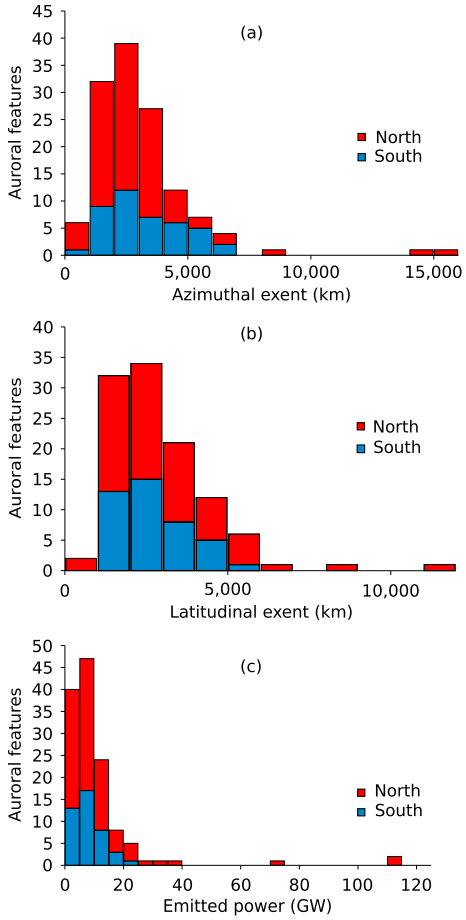

Figure 3. Histograms displaying the distribution of the auroral feature characteristics: (a) azimuthal extent; (b) latitudinal ionospheric extent, both inferred from the auroral UV morphology; and (c) power emitted in the EUV + FUV Lyman and Werner bands by the auroral features selected in the north (red) and in the south (blue). Both azimuthal and radial dimensions range between 640 and 15,300 km. The most probable emitted power of the features is between 5 GW and 10 GW.

at least one auroral feature is present. These emissions are relatively frequent since they are observed on average at least every other day. Specifically, days during which only one auroral feature is observed represent 30% of the cases in the north and 20% in the south. Occasionally, up to eight simultaneous equatorward isolated auroral features are observed both in the northern as well as in the southern hemispheres.

Some of the morphological characteristics of the equatorward auroral structures are displayed in Figure 3. Figures 3a and 3b show the ionospheric azimuthal and radial extents of the auroral features in kilometers. We determine the ionospheric longitudinal and latitudinal extents of the auroral features from the coordinates of the four extreme points of the auroral structure in the northern (red) and in the southern (blue) hemispheres. Both longitudinal and latitudinal dimensions range between 640 and 15,300 km. The largest auroral structure measures 11,700 km latitudinally and 14,400 km longitudinally. The radial and azimuthal extents of the auroral features have the same order of magnitude as the auroral structure's extents associated with the auroral signature of an injection ($6000 \times 15{,}000$ km) observed at Jupiter by *Bonfond et al.* [2012]. This latter structure is included in the present database and represents one of the largest selected structures. Figure 3c shows the power emitted in the extreme ultraviolet (EUV) and far ultraviolet (FUV) Lyman and Werner bands by these auroral features inferred from the conversion coefficients given by *Gustin et al.* [2012]. The power ranges from 2×10^{-2} GW to 113 GW, with the majority of the features characterized by an emitted power between 5 and 10 GW. Significant temporal variations of the power (around 50% between minimum and maximum) are systematically observed in the whole data set. The uncertainty on the count rate and on the background removal was negligible since it is small compared to the inaccuracy of the boundary selection procedure of the auroral features. To estimate this uncertainty, each manually selected pixel forming the contour of the feature is replaced with a random direct neighbor, and we estimate the power inside this new contour. For each feature of the data set, we repeat this operation 100 times, and we compute the standard deviation of the emitted power, which typically lies around 10% of the initial value. The observed fluctuations are larger than the standard deviation. Thus, these variations provide strong evidence that the equatorward auroral features are highly variable. The average time between two consecutive maxima of the emitted power is 8 ± 3 min. Such time scale should be compared with the typical periodicity of 18 min highlighted by *Louarn et al.* [2001] for the energetic events they associate with the injection signatures. This typical periodicity is thus on the same order of magnitude than the average time between two consecutive maxima of the auroral emitted power. These measurements were not concurrent, which could explain a factor of 2 between the two values.

The observed lifetime of each selected auroral UV feature in the northern and in the southern hemispheres is defined as the time range during which each feature is bright enough to be observed with HST, STIS, or ACS (with a sensitivity threshold of a few kilorayleighs, depending on the background level of the planetary disk). The observed lifetime of the auroral features varies between 5 and 213 min. Seventy-one percent of the observed lifetime of the auroral features are between 30 and 50 min corresponding to one orbit time

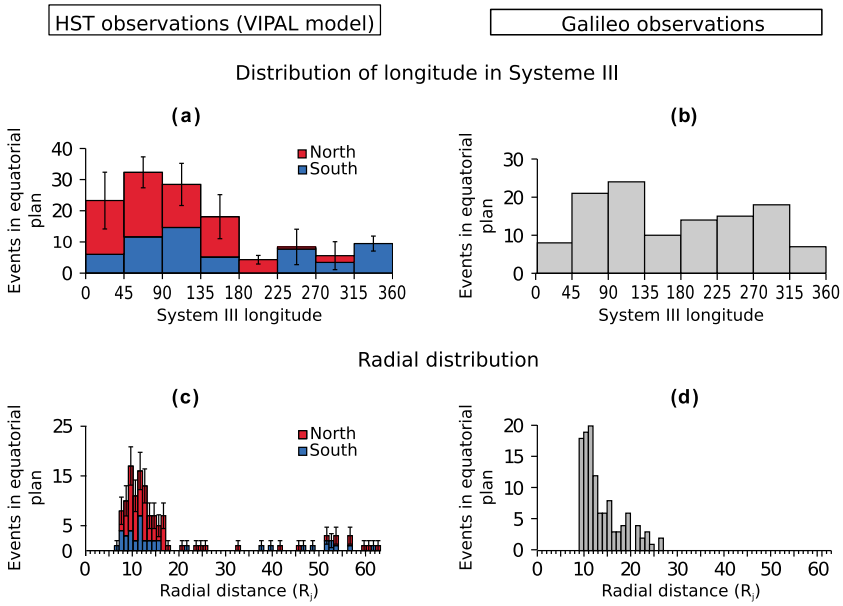

Figure 4. (a) Histogram of the magnetically mapped System III longitude of the auroral features. (b) Histogram of the radial position of the auroral features. The values in the north and in the south are indicated in red and blue, respectively. The error bars are drawn assuming a binomial law for each bin, and they correspond to the standard deviation of the distribution. The most probable radial position of the mapped auroral features is between 10 and 13 R_J. The most probable longitudinal position lies between 45° and 135° in the northern hemisphere and between 45° and 90° in the southern hemisphere. (c) Histogram of the System III longitude of the energetic particle injections detected by Galileo (adapted from *Mauk et al.* [2002]). (d) Histogram of the radial position of the energetic particle injections detected by Galileo (adapted from *Mauk et al.* [2002]). Figures 4c and 4d show that the most probable radial position of the injection events considered by *Mauk et al.* [1999] is between 10 and 12 R_J and they display no preferential longitude.

observation (approximately 45 min). We performed a brightness (emitted power) analysis similar to that of *Radioti et al.* [2009a]. Unfortunately, the results of the analysis are not totally conclusive since, contrary to the Saturn cases presented by *Radioti et al.* [2009a], the lifetime of the auroral structures is longer than the observation. As a result, it is not possible to derive Maxwellian full-width-at-half-maximum lifetimes that could have been directly compared with those obtained by *Radioti et al.* [2009a]. Still, this analysis shows that the phenomenon associated with the auroral structures is taking place for long periods of time, presumably on the order of several hours. If some auroral features have an apparent lifetime shorter than the duration of one HST orbit, this is because they move out of the field of view of the camera before the end of the orbit. In the present data set, we were not able to capture the full life cycle of an equatorward auroral feature in a single orbit. In the very few cases during which several consecutive HST orbits were obtained, auroral signatures persisted throughout the sequence.

2.2. Comparison of Auroral Emissions With In Situ Galileo Observations

The goal of this study is to highlight the common properties between the mapped auroral structures and the plasma injections present in the equatorial plane of Jupiter. To perform this comparison, we magnetically map the center position of the auroral signatures from the ionosphere to the equatorial plane using the VIPAL magnetic field model [*Hess et al.*, 2011]. The VIPAL magnetic field model is a fifth-degree and fifth-order spherical harmonic decomposition of the Jovian magnetic field model. Contrary to earlier models, both the longitude and latitude of the Io UV footprint are used to constrain for the model. VIPAL is particularly suitable for auroral features appearing between the auroral footpaths of Io and Ganymede, which are the regions where most injections studied by *Mauk et al.* [1999] are located. Figures 4a and 4b show the mapped position and radial distance of the auroral features in System III longitude normalized for all System III longitudes in the northern (red) and in the southern (blue) hemispheres. This normalization accounts for an observational bias in the selected database resulting from the limited range of CML, which was adopted to optimize the viewing geometry. To achieve this, the equatorial plane is divided into eight sectors of equal size (45°) with the origin of the first sector set to 0° of System III longitude. The normalization accounts for the number of times

the sectors were observed throughout the database. In each sector, the number of auroral features is divided by this number. All these values are then normalized in such a way that the total number of observed auroral features equals 130. We estimate the probability of the presence of auroral features assuming a binomial distribution and the error bars in Figures 4a and 4b correspond to the standard deviation of the distribution. The magnetospheric source regions of the selected auroral features appear to map at all longitudes and at radial distances between 7 and 62 R_J. The most probable radial position of the mapped auroral features lies between 10 and 13 R_J, and their most likely equatorial longitude lies between 45° and 135°, for the northern features, and between 45° and 90° of equatorial longitude for the southern ones. Only 15% of the cases magnetically map beyond 40 R_J. The latter population should be considered with caution since the VIPAL model becomes increasingly inaccurate beyond Ganymede's orbit. Figures 4c and 4d show the spatial distribution of energetic particle injections identified by Galileo [*Mauk et al*., 1999]. They are present at all System III longitudes, i.e., at no preferential longitude, and at radial distances between ~9 R_J and ~27 R_J. These two distances are the minimum and maximum radial positions sampled by Galileo during the time periods considered in the in situ study of *Mauk et al*. [1999], for which the most probable radial distances were found between 10 and 12 R_J.

Even though HST and Galileo spacecraft observations are not contemporary, their statistical distribution may be compared. When magnetically mapped back in the equatorial plane, the auroral features appear at all System III longitudes and only beyond Io's orbit. These results are consistent with the finding of *Mauk et al*. [2002] concerning injections observed in situ. The main difference between the spatial distribution of events inferred from HST and Galileo stems from their different sampling methods; indeed, HST observations map to a large portion of the dayside magnetosphere, but most of the nightside magnetosphere is out of reach of the telescope. On the other hand, the Galileo spacecraft was obviously not able to sample all local times and all local distances simultaneously. Given the relatively good agreement between HST and Galileo observations (Figure 4), we suggest that the equatorward auroral features that we considered for this study are possibly associated with energetic particle injections in the Jovian magnetosphere. If the auroral structures studied are connected to auroral signatures of injections, the present analysis complement the study of *Mauk et al*. [2002] which was based on one unique case of simultaneous HST and Galileo observations. Assuming that these isolated auroral features are related to plasma injection, this is the first time that injection signatures are observed beyond 27 R_J. The observations made with interplanetary probes, such as Galileo, provide only local properties of the magnetosphere. By contrast, the auroral emissions provide a global picture of the magnetosphere and allow us to perform a more complete statistical study. Importantly in this study, we show, for the first time, that several auroral signatures of injections may be observed simultaneously at different local time sectors, indicating that simultaneous injections may occur at the same time from different locations in the magnetosphere rather than from a unique and localized region in Jupiter's aurora. It should be noted that *Radioti et al*. [2013] reported more than one auroral signature of injection observed simultaneously in Saturn's aurora. In addition, multifluid MHD simulations of Saturn's magnetospheric plasma flows by *Kidder et al*. [2009] are showing several simultaneous events. The presence of simultaneous auroral signatures of injections could be the consequence of the interchange instability, since ideal magnetohydrodynamic numerical simulations, such as those of *Yang et al*. [1994], suggest that the Io torus breaks up into several long fingers implying several injections at different local times in the equatorial plane. Alternatively, simultaneous injections may result from the long lifetime of some events. Indeed, injections are not necessarily created simultaneously. For example, injections successively generated at the same local time sector will rotate with Jupiter and thus appear at different local times on HST images.

3. Plasma Transport, Magnetospheric Structures Studied, and Injections

The location of the equatorial source region of the auroral signatures studied is reported in Figure 5. Figure 5 summarizes the results displayed in Figures 2 and 4 with the location of mapped structures observed in the north (red diamonds) and in the south (blue squares). These auroral features magnetically map between 7 R_J and 62 R_J. For 71% of the cases in the north and 64% of the south ones, the signatures map between the orbits of Io and Ganymede. Only 12% of the cases in the north and 22% in the south are located beyond 40 R_J. The auroral features studied here are never observed inward of the Io footprint. Therefore, the orbit of Io appears as a natural inner boundary for the phenomenon at the origin of the auroral signatures. The phenomenon studied may be related to centrifugal driven interchange events. Such as the inward moving

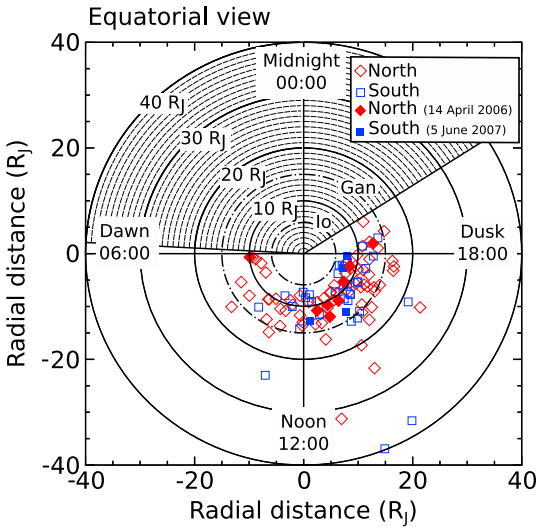

Figure 5. Magnetically mapped local time location of the auroral UV features under study in the equatorial plane. The red diamonds and blue squares show the mapped position of the northern and southern auroral features, respectively. The different circles indicate the radial distance from the orbit of Io to 40 R_J. A wide local time region (dashed region) is not covered by HST images, owing to Earth-based observing geometry. These auroral features magnetically map between 7 R_J and 62 R_J. The local time of the auroral structures covers all values in the sector accessible to HST 06:00 to 20:00 UT. The red filled diamonds indicate the location of eight distinct features observed simultaneously on 4/14/2006 in the northern hemisphere. The blue filled squares indicate the location of four distinct features observed simultaneously on 6/5/2007 in the southern hemisphere.

interchange driven flux tubes balance the outward flux. In this case, the events studied move in as far as the mass loading does, such as the Io's torus is the inner boundary of the phenomenon. From the data set of *Mauk et al.* [1999], this observation could not be made for injections because the minimal radial position sampled by Galileo in Mauk et al.'s study is 9 R_J.

The azimuthal distribution of the magnetospheric structures studied spans a large local time sector from 06 LT to 20 LT. However, it should be noted that a large local time region is not accessible to HST, owing to Earth-based observing geometry constraints (dashed region in Figure 5). We observe 65% of events in the sector between noon and dusk, which represents an average of ~11% of events per local time hour. This is significantly more than in the two other sectors (dawn to noon and dusk to midnight), where we observe on average 4.5% of events per local time hour between dawn and noon and 3% of events per local hour between dusk and midnight. If we consider separately the two hemispheres, we observe a similar behavior.

For approximately 30% of the data set, we observe more than one auroral feature on the same HST orbit. Two particular cases are highlighted with filled diamonds and squares in Figure 5. The first case corresponds to observations made on 14 April 2006 in the northern hemisphere, where eight events are observed simultaneously. The second case corresponds to observations obtained on 5 June 2007 in the southern hemisphere during which four events were simultaneously observed. We observe that the structures are present simultaneously at different local times and at different radial distances. The distribution of longitudes in local time for the whole data set was normalized with the same method as that used in Figure 4 and shown in Figure 6. We observe a relatively uniform distribution of structures mapping to the southern hemisphere. For the northern hemisphere, the most probable longitudes of structures, when mapped in the equatorial plane, lie between 12 LT and 16 LT. However, we note that due to the biased CML distribution in the northern hemisphere, this sector usually corresponds to the same System III longitude range located in the magnetic anomaly of the northern pole at Jupiter. Hence, we assume that the overpopulation in this sector, seen in the northern hemisphere only, is most probably linked to an observational bias associated with the presence of the northern magnetic anomaly that makes it easier to discriminate auroral feature detaching from the rest of the emission.

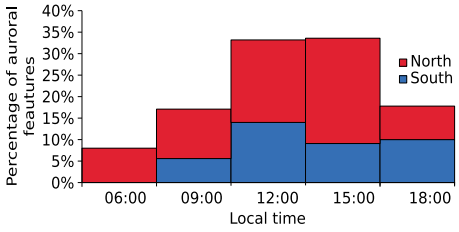

Figure 6. Magnetically mapped local time of the auroral features under study. Observations in the north and south are indicated in red and blue, respectively. The distribution of the mapped structures in the southern hemisphere is relatively uniform in sectors where these structures are visible. The most probable local time sector in the equatorial plane ranges from 12:00 to 18:00 UT in the north.

In situ signatures of recently reconnected and inward moving flux tubes were found at radial distances ranging from 33 to 155 R_J in the tail between 19 and 06 LT [e.g., *Vogt et al.*, 2010; *Kronberg et al.*, 2005]. Such flux tubes would map within the main auroral oval, and their auroral counterparts are thought to be the polar dawn spots

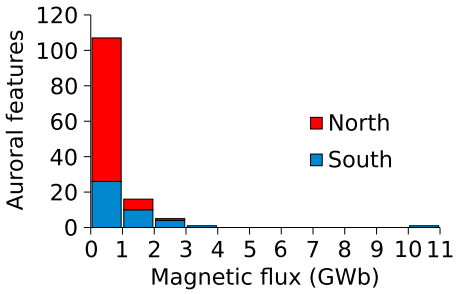

Figure 7. Histogram of the inward magnetic flux associated with auroral features. Contribution from the northern (southern) auroral features is displayed in red (blue).The majority of the auroral features is associated to a magnetic flux between 0.002 GWb and 1 GWb.

[*Radioti et al.*, 2008, 2010]. These structures appear to dissipate within a few (<4) hours as not polar dawn spot has ever been found beyond noon. Alternatively, the low-latitude features discussed in the present paper are seen at all observable local times, which leave us with only two possible explanations. Either the phenomenon causing them, the interchange instability being the most likely one, can take place at any local time, or they could still originate from a privileged local time sector. One possible scenario would be that the interchange instability might be enhanced in a specific local time sector, as a result of some topological reconfiguration subsequent to tail reconnection. But then, the lifetime of the heated plasma bubble has to be significantly longer than 4 h for their auroral signatures to remain equally observable whatever the local time accessible to HST.

Finally, in order to determine the typical radial and azimuthal extents of magnetospheric signatures studied in the equatorial plane, we mapped the coordinates of the four extreme points of each auroral structure in the equatorial plane. The radial extent of the events under consideration ranges between 1 and 10 R_J with the majority (~60%) between 1 R_J and 4 R_J. Their typical azimuthal size is between 0.1 R_J and 7 R_J with the majority (~80%) between 0.1 R_J and 3 R_J.

3.1. Magnetic Flux

During an injection, a parcel of sparse and hot plasma is transported into a region of dense and cold plasma. As heavy plasma moves outward, sparse plasma must be injected inward in the magnetosphere in order to conserve magnetic flux in this region. In the following paragraph, we compare the amount of inward moving magnetic flux associated with the auroral signatures of magnetospheric structures considered in this study with estimations of the outward moving flux.

The inward flux associated with each event is estimated by multiplying the surface magnetic field at the center position of the auroral feature by the area subtended by this auroral emission. Figure 7 shows the magnetic flux associated with each event in the northern (red) and in the southern (blue) hemispheres. The resulting magnetic flux ranges from 1.9×10^{-3} GWb to 10 GWb with the majority (~80%) between 1.9×10^{-3} GWb and 1 GWb. In one case only, the flux reaches a value as high as 10 GWb. The magnetic flux associated with auroral features observed in the south is generally higher than in the north. The median number of injection per day is 1 (see section 2.1) so that the mean magnetic flux is approximately 0.65 GWb per event. In our data set, there is generally only one HST orbit per day, and the auroral features are usually visible for the whole orbit. However, there are 16 cases of two or more consecutive HST orbits. For each of those cases, the auroral features under study are seen at the same System III longitudes all along the sequence. Accordingly, we assume that the typical event duration is at least equal to the maximum observed lifetime (~3 h). With such a typical duration, the mean magnetic flux is ~4.5 GWb and the maximum magnetic flux is ~33.75 GWb within these 3 h. As far as the outward magnetic flux is concerned, a typical value resulting from the transport of iogenic plasma by flux tube interchange may be calculated using the magnetospheric plasma radial transport velocity and the magnetic field magnitude in the equatorial plane.

$$\Phi\mathrm{out}(R,t) = S(t)B(R) \tag{1}$$

$$S(t) = \pi(R + [V_r(R) * t])^2 - \pi R^2 \tag{2}$$

where $S(t)$ is the area covered by the radially moving plasma in the equatorial plane in t seconds, $B(R)$ is the value of the magnetic field at radial distance R, and V_r is the radial plasma outflow speed. According to *Bagenal and Delamere* [2011], at 20 R_J, $V_r(20\ R_J)$ is between 6 km/s and 40 km/s and B~15 nT. Following equations (1) and (2), the estimated outward moving magnetic flux lies between 82.8 and 273.3 GWb/d. This is 1 and 2 orders of magnitude larger, respectively, than the inward magnetic flux inferred from the present auroral analysis. This difference in magnitude may be explained as follows. In the present study, we only considered the auroral features strictly matching our selection criteria for calculating the inward moving flux.

However, every magnetospheric event might not lead to an auroral signature bright enough to be detected; this detection threshold could explain part of the discrepancy. Moreover, only 40% of the auroral region is seen by HST at once, implying that we do not have the ability to observe all auroral features that would have appeared simultaneously. Finally, only ~45 min of an HST orbit may be used to observe Jupiter (the time during which HST is in the shadow casted by the Earth). Assuming that the duration of the auroral signatures is ~3 h (maximum observed lifetime of auroral features in the few sequences of consecutive HST orbits), this implies that HST could have missed three of the signatures that appeared on this particular day. As the observed auroral emissions correspond to 40% of all local time, and if it is hypothesized that the events take place at no preferential longitude, it is reasonable to further multiply the number of observed signatures by 2.5 to obtain the actual total number of magnetospheric structures present at all longitudes. All in all, we estimate a multiplication factor on the order of 8. With such a correction factor, the mean daily magnetic flux becomes ~15 GWb. We note that this flux remains on the low side of the estimated outward flux, meaning that events may account for only 18% of the inward flux. The outward flux must balance the inward flux, and large-scale plasma injections are expected to largely contribute to the latter [*Krupp et al*., 2004]. If the selected auroral features are associated with plasma injections in the magnetosphere, then one would expect the related magnetic flux to at least partly balance the outward flux. Indeed, the values that we derive are on the same order of magnitude, even if our injection-related inward flux is 5 times lower than the outward flux. The underestimation of the inward flux may be, at least in part, related to our five selection criteria of auroral signatures, listed in section 2, which may be too restrictive. Moreover, we cannot exclude that we missed features too faint to be detected.

4. Summary and Conclusions

In the present analysis, we report the first statistical study of Jovian auroral features possibly associated with signatures of magnetospheric injections, based on HST auroral data from 2000 to 2007. Using the VIPAL magnetic field model, we magnetically map the auroral structures in the equatorial plane and we investigate their characteristics. We examine the possibility that the selected UV auroral features are related to injection events in the Jovian magnetosphere. We show that these equatorward auroral features are common as they appear in more than half of the data sample. Most observations displayed only one unquestionable auroral feature per day. We occasionally observe several auroral structures on the same image, pointing out to multiple regions of generation of magnetospheric events instead of a localized source region. Generally, the auroral features are visible during the whole observation orbit, and when several consecutive HST orbits were available, the auroral features were systematically observed during the whole sequence. Accordingly, this strongly suggests that their lifetime is greater than 45 min. Our analysis shows that the auroral features are seen at all System III longitude and preferentially map to distances between 7 R_J and 40 R_J. We compare these HST observations with in situ injection signatures obtained from Galileo energetic particle data, and we demonstrate that the auroral and in situ measurements are present at the same location in the magnetosphere, indicating that the auroral features under study are most probably signatures of injections. We also note that the lifetime of these auroral structures is consistent with the lifetime of the injections. Moreover, the temporal variations of the emitted power have the same typical time scale (8 min) as those of the injections observed in radio domain (18 min) [*Louarn et al*., 2001]. Finally, we estimate the inward moving magnetic flux associated with these auroral signatures and compare it with the outward moving magnetic flux. We estimate that the daily inward moving flux associated with events can account for at least 18% of the outward flux. If the selected structures are signatures of plasma injections in the equatorial plane, then this discrepancy might be the result of too restrictive selection criteria of the auroral features or the underestimation of their lifetime or a problem of detection threshold.

Acknowledgments

This work is based on publicly available observations acquired with the NASA/ESA Hubble Space Telescope and obtained from the Space Telescope Science Institute (https://archive.stsci.edu/hst/search.php; programs GO8657, 10140, 10507, and 10862), which are operated by AURA, Inc., for NASA under contract NAS5-26555. B.B. is supported by the F.R.S.–FNRS. This work was partly funded by the PRODEX Program managed by the European Space Agency in collaboration with the Belgian Federal Science Policy Office.

Michael Liemohn thanks the reviewers for their assistance in evaluating this paper.

References

Bagenal, F., and P. A. Delamere (2011), Flow of mass and energy in the magnetospheres of Jupiter and Saturn, *J. Geophys. Res.*, *116*, A05209, doi:10.1029/2010JA016294.

Bonfond, B., D. Grodent, J. C. Gerard, A. Radioti, V. Dols, P. A. Delamere, and J. T. Clarke (2009), The Io UV footprint: Location, inter-spot distances and tail vertical extent, *J. Geophys. Res.*, *114*, A07224, doi:10.1029/2009JA014312.

Bonfond, B., D. Grodent, J. C. Gérard, T. Stallard, J. T. Clarke, M. Yoneda, A. Radioti, and J. Gustin (2012), Auroral evidence of Io's control over the magnetosphere of Jupiter, *Geophys. Res. Lett.*, *39*, L01105, doi:10.1029/2011GL050253.

Carbary, J. F., T. W. Hill, and A. J. Dessler (1976), Planetary spin period acceleration of particles in the Jovian magnetosphere, *J. Geophys. Res.*, *81*(28), 5189–5195, doi:10.1029/JA081i028p05189.

Cowley, S. W. H., and E. J. Bunce (2001), Origin of the main auroral oval in Jupiter's coupled magnetosphere-ionosphere system, *Planet. Space Sci.*, *49*(10–11), 1067–1088, doi:10.1016/s0032-0633(00)00167-7.

Grodent, D., J. T. Clarke, J. Kim, J. H. Waite Jr., and S. W. H. Cowley (2003a), Jupiter's main auroral oval observed with HST-STIS, *J. Geophys. Res.*, *108*(A11), 1389, doi:10.1029/2003JA009921.

Grodent, D., J. T. Clarke, J. H. Waite Jr., S. W. H. Cowley, J. C. Gerard, and J. Kim (2003b), Jupiter's polar auroral emissions, *J. Geophys. Res.*, *108*(A10), 1366, doi:10.1029/2003JA010017.

Grodent, D., B. Bonfond, J.-C. Gérard, A. Radioti, J. Gustin, J. T. Clarke, J. Nichols, and J. E. P. Connerney (2008), Auroral evidence of a localized magnetic anomaly in Jupiter's northern hemisphere, *J. Geophys. Res.*, *113*, A09201, doi:10.1029/2008JA013185.

Grodent, D., B. Bonfond, A. Radioti, J.-C. Gérard, X. Jia, J. D. Nichols, and J. T. Clarke (2009), Auroral footprint of Ganymede, *J. Geophys. Res.*, *114*, A07212, doi:10.1029/2009JA014289.

Gustin, J., B. Bonfond, D. Grodent, and J. C. Gérard (2012), Conversion from HST ACS and STIS auroral counts into brightness, precipitated power, and radiated power for H_2 giant planets, *J. Geophys. Res.*, *117*, A07316, doi:10.1029/2012JA017607.

Hess, S. L. G., B. Bonfond, P. Zarka, and D. Grodent (2011), Model of the Jovian magnetic field topology constrained by the Io auroral emissions, *J. Geophys. Res.*, *116*, A05217, doi:10.1029/2010JA016262.

Kennelly, T. J., J. S. Leisner, G. B. Hospodarsky, and D. A. Gurnett (2013), Ordering of injection events within Saturnian SLS longitude and local time, *J. Geophys. Res. Space Physics*, *118*, 832–838, doi:10.1002/jgra.50152.

Kidder, A., R. M. Winglee, and E. M. Harnett (2009), Regulation of the centrifugal interchange cycle in Saturn's inner magnetosphere, *J. Geophys. Res.*, *114*, A02205, doi:10.1029/2008JA013100.

Kronberg, E. A., J. Woch, N. Krupp, A. Lagg, K. K. Khurana, and K. H. Glassmeier (2005), Mass release at Jupiter: Substorm-like processes in the Jovian magnetotail, *J. Geophys. Res.*, *110*, A03211, doi:10.1029/2004JA010777.

Krupp, N., J. Woch, A. Lagg, B. Wilken, S. Livi, and D. J. Williams (1998), Energetic particle bursts in the predawn Jovian magnetotail, *Geophys. Res. Lett.*, *25*(8), 1249–1252, doi:10.1029/98GL00863.

Krupp, N., et al. (2004), The dynamics of the Jovian magnetosphere, in *Jupiter. The Planet, Satellites and Magnetosphere*, edited by F. Bagenal, T. E. Dowling, and W. B. McKinnon, Cambrigde Univ. Press, Cambridge, U. K.

Louarn, P., B. H. Mauk, M. G. Kivelson, W. S. Kurth, A. Roux, C. Zimmer, D. A. Gurnett, and D. J. Williams (2001), A multi-instrument study of a Jovian magnetospheric disturbance, *J. Geophys. Res.*, *106*(A12), 29,883–29,898, doi:10.1029/2001JA900067.

Louarn, P., N. Andre, C. Jackman, S. Kasahara, E. Kronberg, and M. Vogt (2014), Magnetic reconnection and associated transient phenomena within the magnetospheres of Jupiter and Saturn, *Space Sci. Rev.*, *1–47*, doi:10.1007/s11214-014-0047-5.

Mauk, B. H., D. J. Williams, and R. W. McEntire (1997), Energy-time dispersed charged particle signatures of dynamic injections in Jupiter's inner magnetosphere, *Geophys. Res. Lett.*, *24*(23), 2949–2952, doi:10.1029/97GL03026.

Mauk, B. H., D. J. Williams, R. W. McEntire, K. K. Khurana, and J. G. Roederer (1999), Storm-like dynamics of Jupiter's inner and middle magnetosphere, *J. Geophys. Res.*, *104*(A10), 22,759–22,778, doi:10.1029/1999JA900097.

Mauk, B. H., J. T. Clarke, D. Grodent, J. H. Watte Jr., C. P. Paranicas, and D. J. Williams (2002), Transient aurora on Jupiter from injections of magnetospheric electrons, *Nature*, *415*(6875), 1003–1005, doi:10.1038/4151003a.

Paranicas, C. P., B. H. Mauk, and S. M. Krimigis (1991), Pressure anisotropy and radial stress balance in the Jovian neutral sheet, *J. Geophys. Res.*, *96*(A12), 21,135–21,140, doi:10.1029/91JA01647.

Radioti, A., D. Grodent, J. C. Gerard, B. Bonfond, and J. T. Clarke (2008), Auroral polar dawn spots: Signatures of internally driven reconnection processes at Jupiter's magnetotail, *Geophys. Res. Lett.*, *35*, L03104, doi:10.1029/2007GL032460.

Radioti, A., D. Grodent, J. C. Gérard, E. Roussos, C. Paranicas, B. Bonfond, D. G. Mitchell, N. Krupp, S. Krimigis, and J. T. Clarke (2009a), Transient auroral features at Saturn: Signatures of energetic particle injections in the magnetosphere, *J. Geophys. Res.*, *114*, A03210, doi:10.1029/2008JA013632.

Radioti, A., A. T. Tomás, D. Grodent, J. C. Gérard, J. Gustin, B. Bonford, N. Krupp, J. Woch, and J. D. Menietti (2009b), Equatorward diffuse auroral emissions at Jupiter: Simultaneous HST and Galileo observations, *Geophys. Res. Lett.*, *36*, L07101, doi:10.1029/2009GL037857.

Radioti, A., D. Grodent, J. C. Gérard, and B. Bonfond (2010), Auroral signatures of flow bursts released during magnetotail reconnection at Jupiter, *J. Geophys. Res.*, *115*, A07214, doi:10.1029/2009JA014844.

Radioti, A., D. Grodent, J. C. Gerard, M. F. Vogt, M. Lystrup, and B. Bonfond (2011), Nightside reconnection at Jupiter: Auroral and magnetic field observations from 26 July 1998, *J. Geophys. Res.*, *116*, A03221, doi:10.1029/2010JA016200.

Radioti, A., E. Roussos, D. Grodent, J. C. Gérard, N. Krupp, D. G. Mitchell, J. Gustin, B. Bonfond, and W. Pryor (2013), Signatures of magnetospheric injections in Saturn's aurora, *J. Geophys. Res. Space Physics*, *118*, 1922–1933, doi:10.1002/jgra.50161.

Siscoe, G. L., and D. Summers (1981), Centrifugally driven diffusion of logenic plasma, *J. Geophys. Res.*, *86*(A10), 8471–8479, doi:10.1029/JA086iA10p08471.

Southwood, D. J., and M. G. Kivelson (1987), Magnetospheric interchange instability, *J. Geophys. Res.*, *92*(A1), 109–116, doi:10.1029/JA092iA01p00109.

Thomsen, M. F. (2013), Saturn's magnetospheric dynamics, *Geophys. Res. Lett.*, *40*, 5227–5344, doi:10.1002/2013GL057967.

Thorne, R. M., T. P. Armstrong, S. Stone, D. J. Williams, R. W. McEntire, S. J. Bolton, D. A. Gurnett, and M. G. Kivelson (1997), Galileo evidence for rapid interchange transport in the Io torus, *Geophys. Res. Lett.*, *24*(17), 2131–2134, doi:10.1029/97GL01788.

Vasyliūnas, V. M. (1983), Plasma distribution and flow, in *Physics of the Jovian Magnetosphere*, edited by A. J. Dessler, pp. 395–453, Cambridge Univ. Press, New York.

Vogt, M. F., M. G. Kivelson, K. K. Khurana, S. P. Joy, and R. J. Walker (2010), Reconnection and flows in the Jovian magnetotail as inferred from magnetometer observations, *J. Geophys. Res.*, *115*, A06219, doi:10.1029/2009JA015098.

Yang, Y. S., R. A. Wolf, R. W. Spiro, T. W. Hill, and A. J. Dessler (1994), Numerical simulation of torus-driven plasma transport in the Jovian magnetosphere, *J. Geophys. Res.*, *99*(A5), 8755–8770, doi:10.1029/94JA00142.